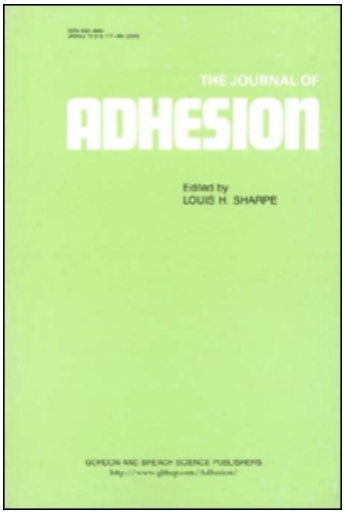

The Journal of Adhesion

Publication details, including instructions for authors and subscription information:
http://www.informaworld.com/smpp/title~content=t713453635

Bond strength measurement between glass fibres and epoxy resin at elevated temperatures using the pull-out and push-out techniques

E. Mäder[a]; S. Zhandarov[a]; S. L. Gao[a]; X. -F. Zhou[b]; S. R. Nutt[b]; S. Zhandarov[c]
[a] Institute of Polymer Research Dresden, Dresden, Germany [b] Center for Composites, University of Southern California, Los Angeles, CA [c] Metal-Polymer Research Institute, National Academy of Sciences of Belarus, Gomel, Republic of Belarus

Online publication date: 08 September 2010

The Journal of Adhesion, 78: 547–569, 2002

0021-8464/02 $12.00 +.00
DOI: 10.1080/00218460290010313

BOND STRENGTH MEASUREMENT BETWEEN GLASS FIBRES AND EPOXY RESIN AT ELEVATED TEMPERATURES USING THE PULL-OUT AND PUSH-OUT TECHNIQUES

E. Mäder
S. Zhandarov
S. L. Gao
Institute of Polymer Research Dresden, Dresden, Germany

X.-F. Zhou
S. R. Nutt
Center for Composites, University of Southern California, Los Angeles, CA

S. Zhandarov
Metal-Polymer Research Institute of the National Academy of Sciences of Belarus, Gomel, Republic of Belarus

Pull-out and push-out measurements were performed on glass fibres in an epoxy resin to determine the dependence of bond strength on test temperature and on fibre surface treatment. A comparative analysis of the two techniques was carried out to elucidate elementary processes of polymer–fibre debonding and to determine energy values for adhesional bonds. Differences in bond strength values for pull-out and push-out tests were attributed to failure mechanisms that were either interface-controlled or matrix-controlled. Evidence for the different failure mechanisms characteristic of the two test techniques was provided by an estimation of failure parameters, such as the activation energy for debonding. Failure mechanisms also were manifest in AFM images, showing differences in topography and roughness that depended on fibre surface treatment, test geometry, and test temperature.

Received 5 September 2001; in final form 21 December 2001.

This is one of a collection of papers honoring Hatsuo (Ken) Ishida, the recipient in February 2001 of *The Adhesion Society Award for Excellence in Adhesion Science, Sponsored by 3M*.

Address correspondence to Edith Mäder, Institute of Polymer Research Dresden, Hohe Strasse 6, D-01069 Dresden, Germany. E-mail: emaeder@ipfdd.de

Keywords: Epoxy resin/glass fibre composites; Micromechanical tests; Bond strength; Activation energy; Atomic force microscopy; Surface roughnes

INTRODUCTION

The pull-out test [1, 2] and the push-out test [3, 4] are popular micromechanical techniques for measuring the bond strength in polymer-fibre composites. In the pull-out test, one end of a fibre is embedded into a matrix block, and the load required to produce interfacial shear is measured (Figure 1a). In the push-out test, a thin transverse section of a unilateral fibrous composite is prepared, and the force required to push out a single fibre fragment (Figure 1c) is determined. The data from these tests are then used to calculate such interfacial parameters as the average or apparent interfacial shear strength, the ultimate interfacial shear strength, τ_{ult} [5, 6], and the critical energy release rate, G_{ic} [7, 8].

These two tests are characterized by substantially different patterns of interfacial loading. In the pull-out test geometry, the interface is subjected to combined shear and tensile load [8], while in the push-out test, the interfacial load involves shear, compression, and frictional components [9]. Therefore, a comparison of the results from these tests provides valuable information about the interface behaviour under different load patterns. In particular, we have shown in our previous paper [9] that in the case of good interfacial bonding (fibre with special sizing improving adhesion), the pull-out test gave greater τ_{ult} and G_{ic} values than the push-out test: strong brittle interfaces can carry greater load in tension than in compression.

The measurement of interfacial parameters at different temperatures can also be useful to predict the interfacial behaviour during application. In this way, we can not only follow the strength variations of the matrix and the interface but also observe transitions between interface-controlled and matrix-controlled failure [10]. However, the most interesting possibility of micromechanical tests at different temperatures is, in all probability, the study of elementary processes of interfacial bonding/debonding and the estimation of their energy characteristics, such as activation energy. For example, in Pisanova et al. [11] the bond strength in polymer-fibre systems was measured as a function of the temperature of the adhesion contact formation. It was found that activation energy values for adhesional bonding differed considerably for different polymer-fibre pairs, due to different mechanisms controlling interfacial bonding between a polymer and a solid surface, viscous flow of a polymer melt, or kinetics of local bond formation. In turn, carrying out micromechanical experiments with

different test techniques should provide information on elementary processes of polymer-fibre debonding (breakage of adhesional bonds) and, in particular, on the energy values for local adhesional bonds between a polymer and a fibre substrate.

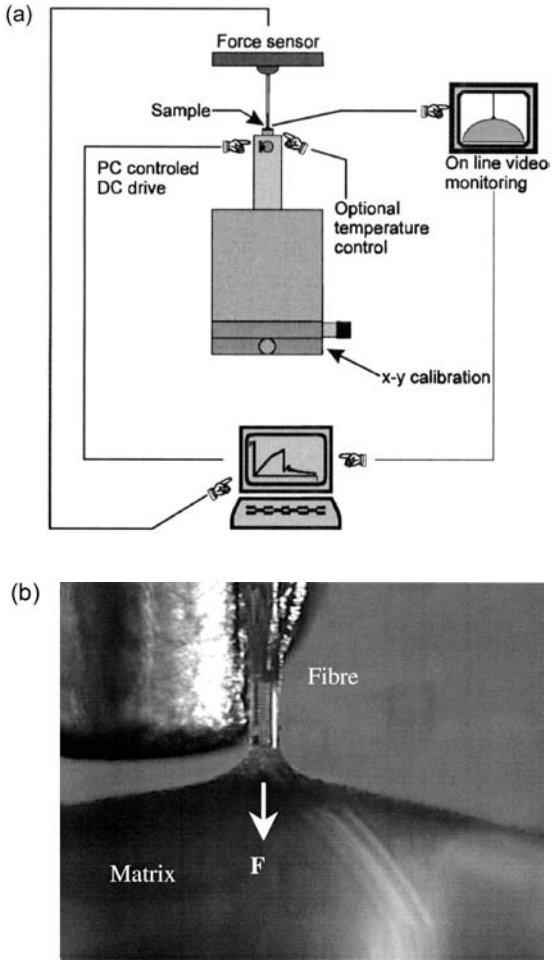

FIGURE 1 (a) Schematic of the single fibre pull-out apparatus. (b) Single fibre embedded in epoxy resin, fibre fixed on the steel rod of force measuring unit. (c) Schematic of the push-out test apparatus. (d) SEM image of the diamond tip pushing out a fibre. (e) Different stages of pushed out fibres. (f) Schematic of the "carbon-fibre indenter" used for temperature-controlled push-out of the fibres for AFM investigation.

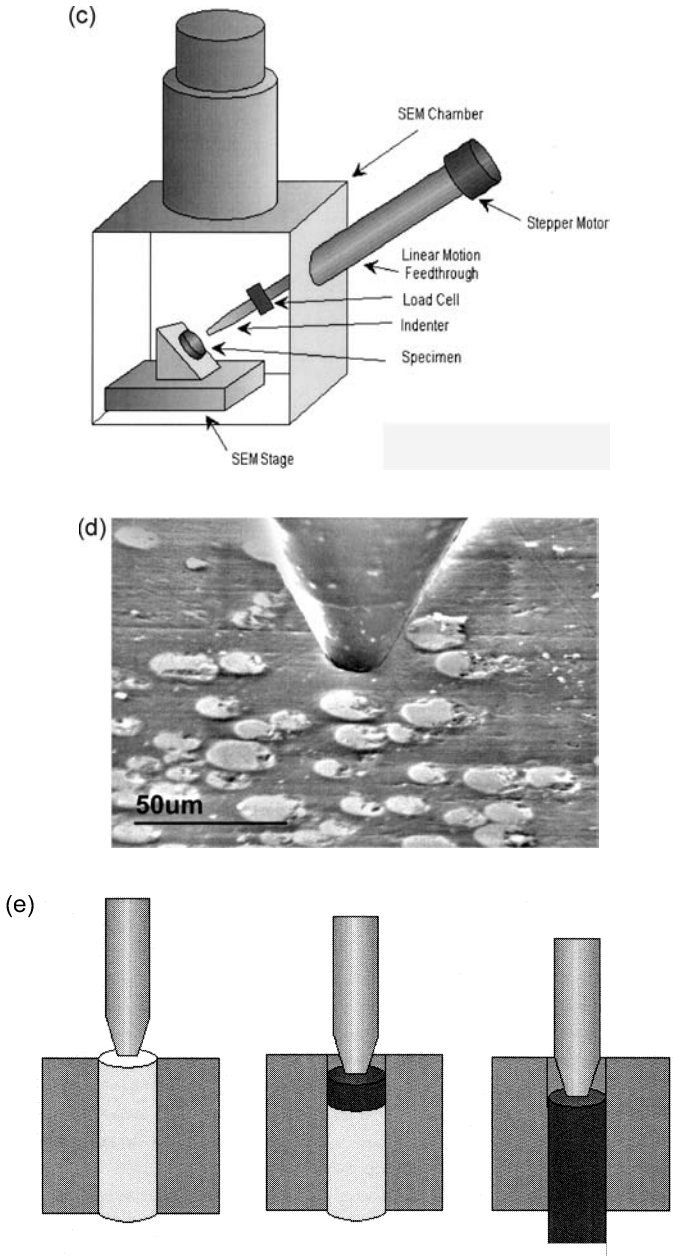

FIGURE 1 (*continued*).

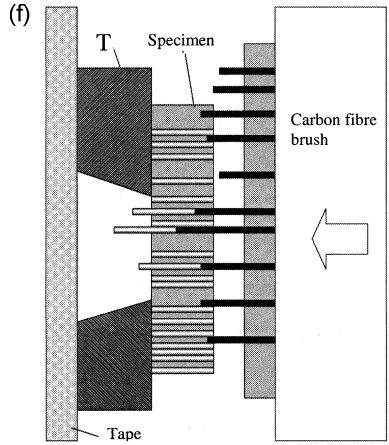

FIGURE 1 (*continued*).

EXPERIMENTAL

E-glass fibres with diameters of about 12 μm, spun at the Institute of Polymer Research Dresden were selected for tests. We used unsized fibres (spun with distilled water in the sizing applicator) as well as those treated by γ-aminopropyltriethoxysilane (APS, sized) during continuous spinning. Diameters of individual fibres were measured microscopically before pull-out testing and by scanning electron microscopy (SEM) during push-out testing. The matrix material was a commercial DGEBA-based, epoxy resin Rütapox L20 and the curing agent Rütapox SL, used in 100:34 weight ratio (manufacturer: BAKELITE AG, Duisburg, Germany). The curing conditions used in this study were similar to those recommended by the manufacturer (6 h, 80°C).

Single Fibre Pull-out Test

Pull-out tests were carried out using a pull-out apparatus made at the Institute of Polymer Research Dresden (Figure 1a, b), which features high-precision fibre displacement (1 μm) and force measurement (1 mN) to generate force-displacement curves and manage data. Single fibres were perpendicularly end-embedded in the matrix resin using time- and temperature-controlled equipment. The embedded lengths were in the range of 50 to 150 μm. The pull-out test was performed at a crosshead displacement rate of 0.01 μm/s. The single fibre composite was heated to

the corresponding temperature using a micro-heater below the sample carrier before the fibre was fixed to the steel rod of the force measuring unit. From each force-displacement curve, the maximum force, $F_{\max}$, and the embedded length, l_e,were determined, and the apparent bond strength, τ_{app}, was calculated for each specimen using the equation

$$\tau_{\text{app}} = \frac{F_{\max}}{\pi d l_e}, \tag{1}$$

where d is the fibre diameter. About 15 to 20 load-displacement curves were evaluated for each fibre/matrix system.

In this traditional data reduction scheme, the interface fracture in micromechanical tests is considered to occur instantaneously, and the maximum external force applied to the fibre is taken to correspond to the onset of debonding. However, at some force F_d (smaller than $F_{\max}$), initial fibre debonding from the matrix may occur, and further increase of the external load with interfacial crack propagation may be attributed to frictional forces in the debonded region. These forces may increase with the debonded area. This introduces complexity in the interpretation of micromechanical test data, and the intricate fracture pattern in the pull-out tests has led some researchers to doubt that the fiber-matrix bond strength can be measured by these tests. Another approach can be used to estimate quantitatively the quality of interfacial bonding from force-displacement curves obtained in pull-out experiments. In this approach, the ultimate interfacial shear strength, τ_{ult}, is given by [5, 6]

$$\tau_{\text{ult}} = \frac{F_d \beta}{\pi d \tanh(\beta l_e)} + \tau_{\text{therm}} \tanh(\beta l_e/2), \tag{2}$$

where β is the shear-lag parameter as defined by Nayfeh [12], and τ_{therm} is defined as

$$\tau_{\text{therm}} = E_f \beta d(\alpha_m - \alpha_f)\Delta T/4, \tag{3}$$

where E_f is the fibre tensile modulus, α_m and α_f are coefficients of thermal expansion of the matrix and the fibre, respectively, and ΔT is the difference between the test temperature and the stress-free temperature.

The ultimate bond strength is usually associated with interfacial adhesion for a given fibre/matrix pair and depends neither on geometrical conditions of the specimen nor on thermal stresses of bond formation.

It should be noted that for the Rütapox epoxy resin, nonlinear behaviour was evident from the general shape of the force-displace-

ment plots. In these cases, calculated τ_{ult} values can be reasonably accurate, although the use of a linear elastic approximation to fit the maximum load value (F_{max}) results in an overestimation of interfacial friction for such specimens.

Push-out Tests

The procedure for preparation of push-out specimens is as follows. E-glass fibres were cut, aligned, and placed in a plastic container $12 \times 12 \times 3\,mm^3$ lined with aluminium foil. Next, the mixture of liquid resin components was poured into the container and the container was placed in an oven for curing at 80°C for 6 h. After curing, thin slices were cut perpendicular to the fibre axis and hand-polished to $\sim 100\,\mu m$. The specimen thickness (embedded fibre length) was measured using SEM before or after the push-out tests (with the sample turned 90 degrees, presenting the cross section).

Single-fibre push-out tests were conducted using a SEM equipped with a screw-driven testing machine that included a 1000 gram load cell. The schematic of the test apparatus is shown in Figure 1c. A conical diamond indenter tip with a 6-μm-diameter flat bottom was fixed onto a tube threaded to the load cell. The 3-axis sample stage was translatable with an accuracy of better than 1 μm, facilitating alignment of the test fibre and the diamond tip. A hot stage was installed under the specimen, enabling controlled heating of test specimens up to 1000°C. In the push-out test, load and displacement data were controlled and recorded. A real-time curve for the dependence of load on indenter displacement was displayed during the test. Figure 1d shows a SEM image of the diamond tip pushing out a selected fibre, and in Figure 1e different stages of pushed-out fibres are schematically shown. About 20 load-displacement curves were obtained for each composite specimen.

Atomic Force Microscopy (AFM)

Topography and roughness

An AFM (a Digital Instruments D3100) was used as both a surface imaging tool and an indentation device to evaluate the nanoscale response of polymer samples. The topography of samples was studied in Tapping Mode. Images consisted of 512×512 pixels, and the scanning frequency was 1 Hz. A silicon cantilever with normal spring constant of 1.5 to 6.3 N/m and a tip radius of 5–10 nm was used. A piezo stack excited the cantilever's substrate vertically, causing the tip to bounce up and down at its resonant frequency of 65.6 kHz with drive

amplitude 200 mV. As the cantilever bounced vertically, the reflected laser beam revealed information about the vertical height of the sample surface. For all samples, several images were recorded at different locations to verify the reproducibility of the observed features.

Four roughness parameters are derived from ASME B46.1 (Surface Roughness, Waviness, and Lay) available from the American Society of Mechanical Engineers, namely, image mean roughness (R_a), maximum height roughness (R_{max}), surface difference, and skewness. Skewness is a nondimensional quantity to measure the symmetry of original surface data about a mean data profile in the cursor box (about 2000 nm^2) without application of plane fitting or flattening. The effective surface area is represented by image surface area difference between surface areas and projected surface areas compared, determined by the following equation:

$$\text{Image surface area difference} = \left[\frac{\sum(\text{area}_{\text{surface},j})}{\sum(\text{area}_{\text{projected},j})} - 1\right] \cdot 100\%. \quad (4)$$

To characterize the fracture surfaces of the embedded fibres after pull-out, the fibres were attached to a pressure sensitive tape on the sample carrier for investigation of both original and debonded regions of the fibre surface. The pushed-out fibres were collected on a tape after pushing out by using a special "carbon-fibre indenter" (cf. Figure 1f). The roughness values determined represent average data for 2 to 4 specimens in 4 μm^2 at every condition.

RESULTS AND DISCUSSION

Figure 2 presents plots of the apparent bond strength, τ_{app}, versus test temperature, T, for the push-out (Figure 2a) and pull-out (Figure 2b) tests. As seen from Figure 2, the adhesion strength for sized fibres was in all cases greater than that for unsized ones. The τ_{app} values decreased with temperature for both unsized and sized fibres tested in both tests. The decrease was fast and rather uniform for all specimens, except for the unsized fibres in the push-out test. This behaviour is discussed below in more detail.

As is known, the value of the apparent bond strength depends in a complex manner on both adhesion and friction at the fibre-matrix interface. However, when tests are performed for the same polymer–fibre system in a narrow range of embedded lengths, the contribution of interfacial friction can be considered, as a first approximation, as proportional to the adhesional strength. Therefore, the behaviour of the ultimate (local) interfacial shear strength, τ_{ult}, which characterizes

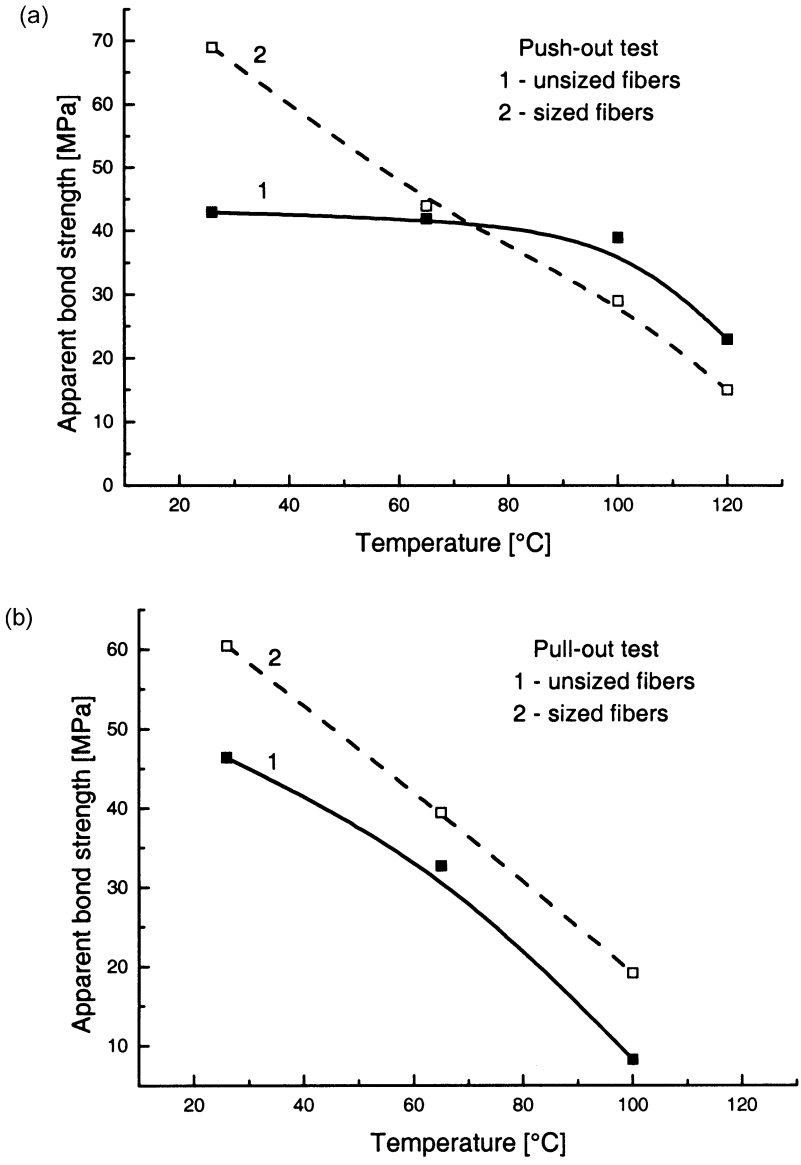

FIGURE 2 Bond strength in the glass fibre–epoxy system at different test temperatures: push-out test, apparent IFSS (a); pull-out test, apparent IFSS (b); pull-out test, ultimate IFSS (c).

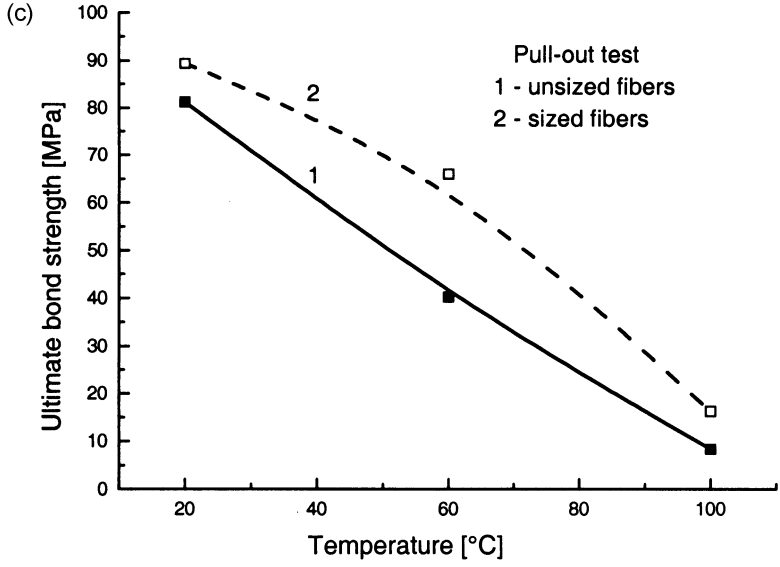

FIGURE 2 (*continued*).

the true strength of adhesional bonds at the interface, is expected to be qualitatively similar to that of τ_{app}. This is confirmed by Figure 2c, in which τ_{ult} is presented as a function of test temperature. Note that the τ_{ult} values in Figure 2c were calculated using the actual elastic moduli of the matrix at different test temperatures, taking into account both "elastic" and "thermal shrinkage" terms in the expression for the ultimate bond strength. The term due to thermal shrinkage appeared to be practically negligible for all test temperatures except room temperature, since the temperature of specimen preparation (80°C) differed only slightly from the test temperatures. Moreover, the elastic term appeared to be much greater than the shrinkage term, even at room temperature.

Similar behaviour of the adhesional strength as a function of temperature for sized and unsized fibres was reported by Wimolkiatisak and Bell [10]. They used electrocopolymerization to coat Hercules AS4 graphite fibres with acrylonitrile/methyl acrylate/acrylic acid, acrylonitrile/methyl acrylate, and glycidyl-acrylate/acrylonitrile interlayers and then measured the effective IFSS, τ_e, in graphite fibre–Epon 828® epoxy systems using the classic version of the fragmentation test (Kelly–Tyson [13]). Their typical result is shown in Figure 3. The behaviour they reported for τ_e was similar to that of τ_{app} in our push-out tests on glass fibre/epoxy specimens. Wimolkiatisak and Bell

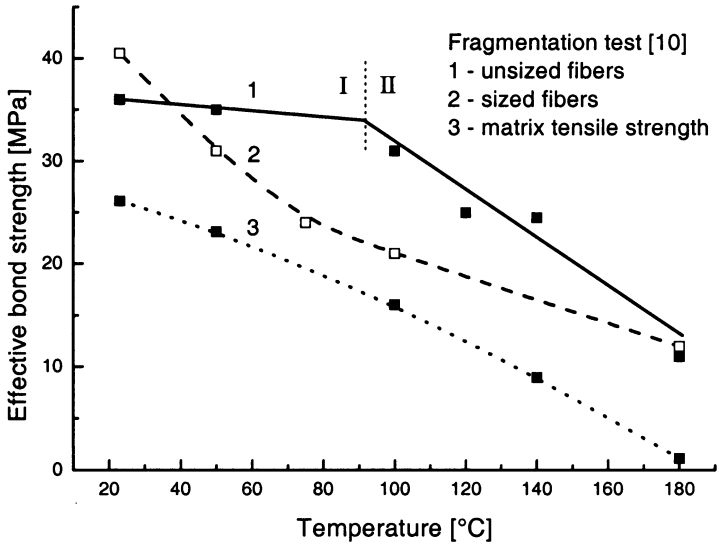

FIGURE 3 Effective bond strength in the graphite fibre–epoxy system at different test temperatures, measured using the fragmentation test [10]. The matrix tensile strength as a function of temperature is also shown.

distinguished two distinctive regions, I and II, in their plot for uncoated samples. They believed that in Region I τ_e remained approximately constant as the temperature was increased (matrix strength was decreased—see curve 3 in Figure 3). In Region II, τ_e decreased with increasing temperature, parallel to the matrix strength loss. Therefore, the authors suggested that the failure was interface-controlled in Region I and matrix-controlled in Region II. (For coated samples, they considered the failure to be interface-controlled for the whole temperature range). While data presented here show that their interpretation is plausible, the pull-out specimens show a different behaviour. In all probability, this is due to different failure mechanisms characteristic of, on the one hand, fragmentation and push-out tests, and, on the other hand, the pull-out test. In our previous paper [9], we discussed the fracture surfaces of glass fibres before and after pull-out at ambient temperatures. Additional experimental proof at elevated temperatures in the form of AFM fractographs for both pull-out and push-out fibres will be presented below. The representative microphotographs (Figures 4 and 5) are markedly different for the two test methods and are also affected by test temperature and by sizing. There are a few points of interest to highlight from the results.

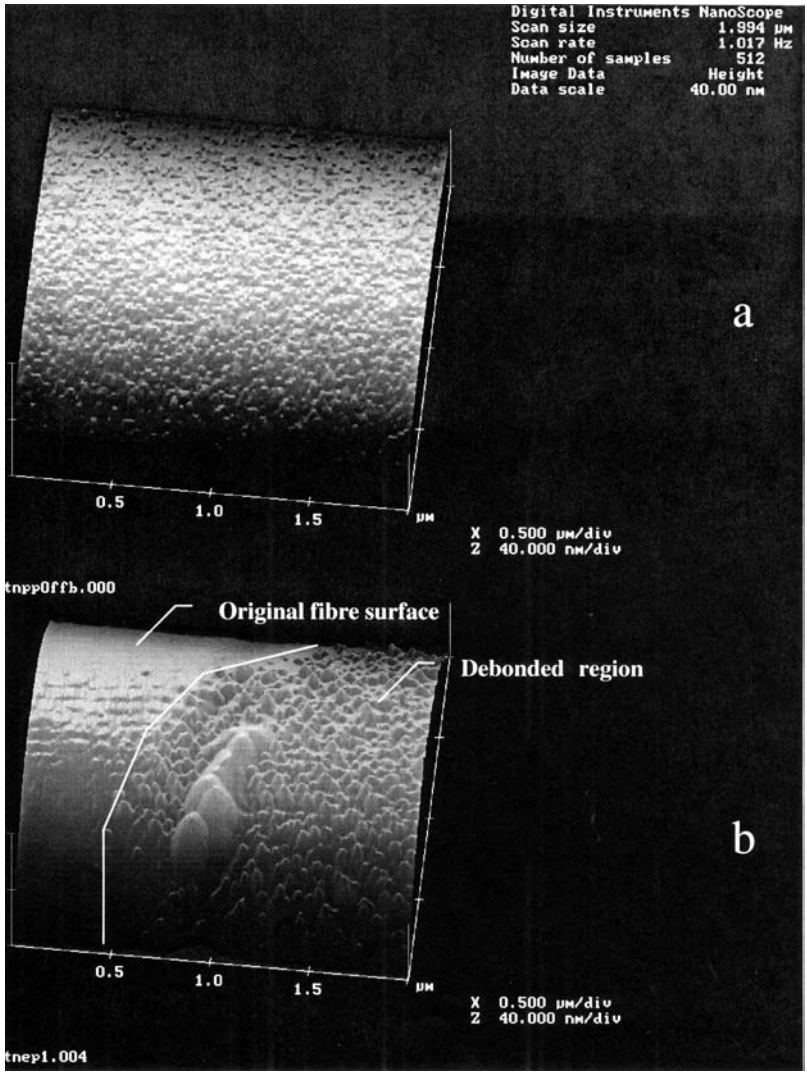

FIGURE 4 Three-dimensional AFM images of fracture surfaces of unsized glass fibre pulled-out at room temperature (a) and APS-sized glass fibre pulled-out at a temperature of 100°C (b).

In pull-out tests, the unsized glass fibre/epoxy specimens (Figure 4a) were characterised by a very smooth fracture surface ($R_a = 0.2$ nm, $R_{max} = 6.5$ nm), which is evidence for a thin interphase in this case. In sharp contrast, a rather thick interphase between sized fibre and

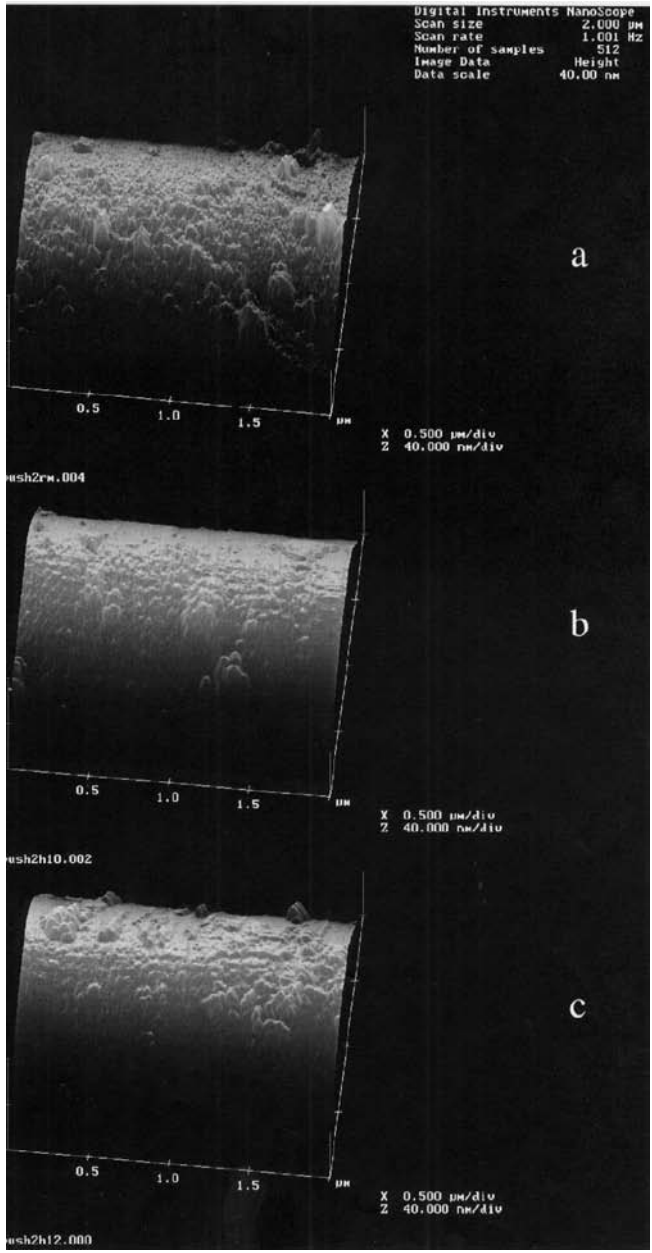

FIGURE 5 Three-dimensional AFM images of fracture surfaces of unsized glass fibres pushed-out at temperatures of (a) 25°C, (b) 100°C, and (c) 120°C.

epoxy was effectively involved in load transfer (Figure 4b). The interphase polymer within 100 to 200 nm of the fibre surface [14] appears to have been extensively stretched during the process of fibre pull-out. The roughness ($R_a = 3.3$ nm, $R_{max} = 54.0$ nm) of the pull-out section is much greater than that of the original fibre surface, indicating cohesive failure within the interphasial region. A qualitative picture of the failure is that it may occur by disentanglement, failure of the polymer chains, and debonding of the chains from the fibre surface.

The fracture surfaces of the fibre after push-out exhibit average and maximum height roughness values slightly larger than those of the sized fibres after pull-out (Figures 5 and 6, Table 1). All the push-out fibre fracture images were dominated by extensive plastic deformation of the matrix along with fibre-matrix interfacial debonding.

With increasing push-out temperature, the roughness data and image surface differences reduced to about one-half or one-fourth, somewhat higher asymmetric and convex Z-data of the fracture surface was suggested based on the increased skewness values (from 1.1 to 2.2). The measured lower interfacial bond strength at elevated temperatures compared with the same systems at ambient temperature is probably due, in large part, to higher ductility within the interphase region due to lower yield strength of the polymer at higher temperature. Moreover, the decrease of interfacial bond strength at either high temperature for the same system or unsized fibres compared with sized fibres might also result in the lack of extensive neighbouring matrix deformation which was replaced by an enhanced fraction of interfacial debonding at low stress level. Nevertheless, the fracture surfaces of sized fibres revealed more than doubled roughness compared with unsized ones due to strong interfacial adhesion (Figure 6, Table 2).

TABLE 1 Fracture Surface Features of Pushed Out Unsized and Sized Glass Fibres Under Various Thermal Conditions

	Temperature of Push-out Test					
	25°C		100°C		120°C	
Fracture surface features	Unsized	Sized	Unsized	Sized	Unsized	Sized
Image mean roughness, R_a (nm)	2.7	5.6	1.0	4.5	1.0	2.1
Maximum height roughness, R_{max} (nm)	41.4	106.5	18.4	61.4	20.0	33.5
Skewness	1.1	1.2	1.3	1.1	2.2	1.1
Image surface difference (%)	3.6	0.9	0.1	2.5	0.0	0.2

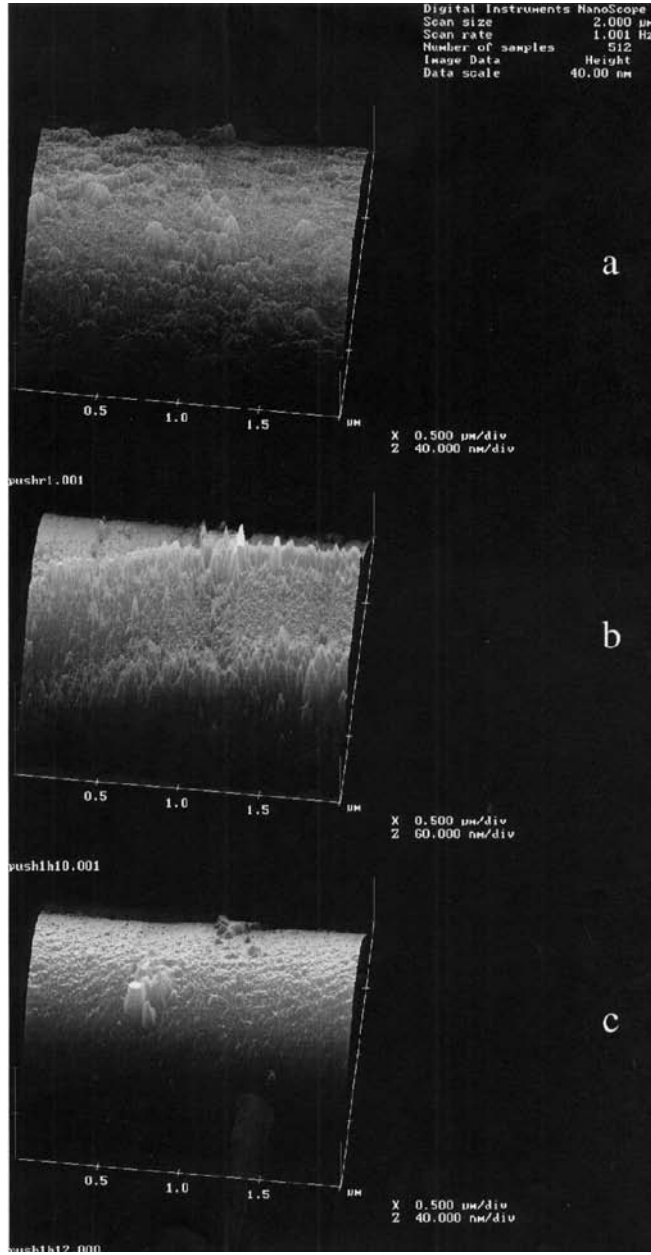

FIGURE 6 Three-dimensional AFM images of fracture surfaces of APS-sized glass fibres pushed-out at temperatures of (a) 25°C, (b) 100°C, and (c) 120°C.

TABLE 2 Activation Energies and Structure-Sensitive Parameters For Fibre–Epoxy Systems

Fibre	Test applied	Sizing	Slope s, MPa/K	γ, m^3	$\gamma^{1/3}$, Å	Activation energy, U_0 kJ/mol	eV
Glass	Push-out	Sized	-0.56	$8.5 \cdot 10^{-28}$	9.5	121	1.25
		Unsized ($T < 100$°C)	-0.054	$8.8 \cdot 10^{-27}$	20.6	314	3.25
		Unsized ($T > 100$°C)	-0.80	$6.0 \cdot 10^{-28}$	8.4	121	1.26
Glass	Pull-out	Sized	-0.56	$8.5 \cdot 10^{-28}$	9.5	117	1.21
		Unsized	-0.51	$9.4 \cdot 10^{-28}$	9.8	113	1.17
Glass	Pull-out[a]	Sized	-0.93	$5.2 \cdot 10^{-28}$	8.0	113	1.17
		Unsized	-0.86	$5.6 \cdot 10^{-28}$	8.2	111	1.15
Graphite	Fragmentation [10]	Coated	-0.17	$2.9 \cdot 10^{-27}$	14.3	154	1.60
		Uncoated (region I)	-0.058	$8.8 \cdot 10^{-27}$	20.6	279	2.89
		Uncoated (region II)	-0.25	$2.0 \cdot 10^{-27}$	12.7	151	1.57
—	—	Matrix strength	-0.16	$3.2 \cdot 10^{-27}$	14.7	144	1.49

[a] Calculated using the ultimate IFSS values.

In the pull-out test, the interfacial load is a combination of tension and shear (pure tension for crack initiation, with increasing contribution of shear at advanced stages of testing) [12, 15]. In contrast, during the fragmentation and push-out test the fibre–matrix interface is loaded in shear combined with *compression*. Therefore, in some cases (at certain test temperatures), where the matrix is "unzipping" from the fibre in the pull-out test, the specimen can only fail through matrix shear yielding in the push-out and fragmentation tests.

Further evidence for these different failure mechanisms is provided by an estimation of the activation energy and the "structure-sensitive parameter" for the failure processes. In the following analysis, we used Zhurkov's theory of long-term strength of polymer materials [16–21]. This theory considers the failure of solids, including polymers, as a relaxation process. The failure is assumed to be initiated by thermal fluctuations in the material; at the site where thermal fluctuation exceeds the energy of a cohesional bond, the bond breaks. The basic equation of this theory (Zhurkov equation) expresses the time-to-failure, t, of a polymer specimen loaded by a stress, σ, as

$$t = t_0 \exp\left(\frac{U_0 - \gamma\sigma}{kT}\right), \tag{5}$$

where k is Boltzmann's constant; U_0, t_0, and γ are parameters that determine the behaviour of the polymer material under load; t_0 is the effective time of activation processes, close to the characteristic time of thermal oscillations of atoms in solids ($\sim 10^{-13}$ s for most solids); U_0 is the activation energy for the failure; and γ is a so-called "structure-sensitive parameter" whose physical meaning will be discussed below. Equation (5) can also be used for the analysis of adhesional failure in heterogeneous systems, such as specimens for micromechanical destructive tests. Substituting the adhesional strength, τ (ultimate or apparent value), for σ in Equation (5), we obtain

$$\tau = \frac{U_0}{\gamma} - \frac{k}{\gamma}\ln\frac{t}{t_0}\cdot T \tag{6}$$

or

$$\tau = \frac{U_0}{\gamma} + s \cdot T, \tag{7}$$

where

$$s = -\frac{k}{\gamma}\ln\frac{t}{t_0}. \tag{8}$$

In Equation (8), t is the duration of a pull-out or push-out test, which is typically several seconds to several minutes. Because the t variation is over two orders of magnitude (from 30 to 3000 s) and $t_0 \approx 10^{-13}$ s, the value of $\ln(t/t_0)$, and, consequently s, varies by only 12%. Therefore, as a first approximation, we can take $s \approx$ const and use $t \approx 10^3$ s as the test duration. Then, having plotted the adhesional strength, τ, as a function of temperature (straight line, according to Equation (8)), we can find γ from the slope, s,

$$\gamma = -\frac{k}{s}\ln\frac{t}{t_0}, \tag{9}$$

and the intercept, $\tau(0)$, on the T axis which yields the activation energy

$$U_0 = \tau(0)\gamma = -\tau(0)\frac{k}{s}\ln\frac{t}{t_0}. \tag{10}$$

The $\tau(T)$ plots for the graphite-Epon 828 pair from Wimolkiatisak and Bell [10] as well as for our glass-epoxy systems are shown in Figure 3 and Figure 7a–d, respectively. The calculated U_0 and γ values are presented in Table 2.

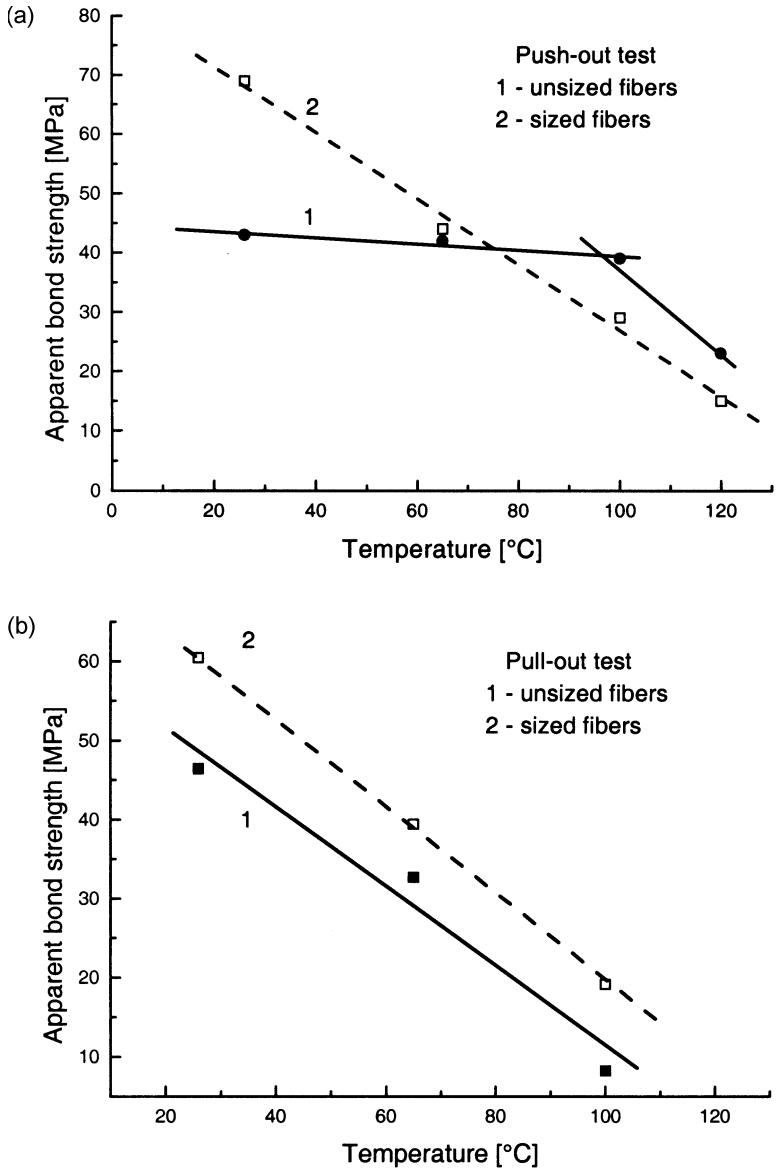

FIGURE 7 Temperature dependencies of the bond strength between glass (a–c) and graphite (d) fibres and an epoxy matrix approximated by straight lines corresponding to Zhurkov's equation: push-out test, apparent IFSS (a); pull-out test, apparent IFSS (b); pull-out test, ultimate IFSS (c); fragmentation test, effective IFSS (calculated using the data reported in Wimolkiatisak and Bell [10]) (d).

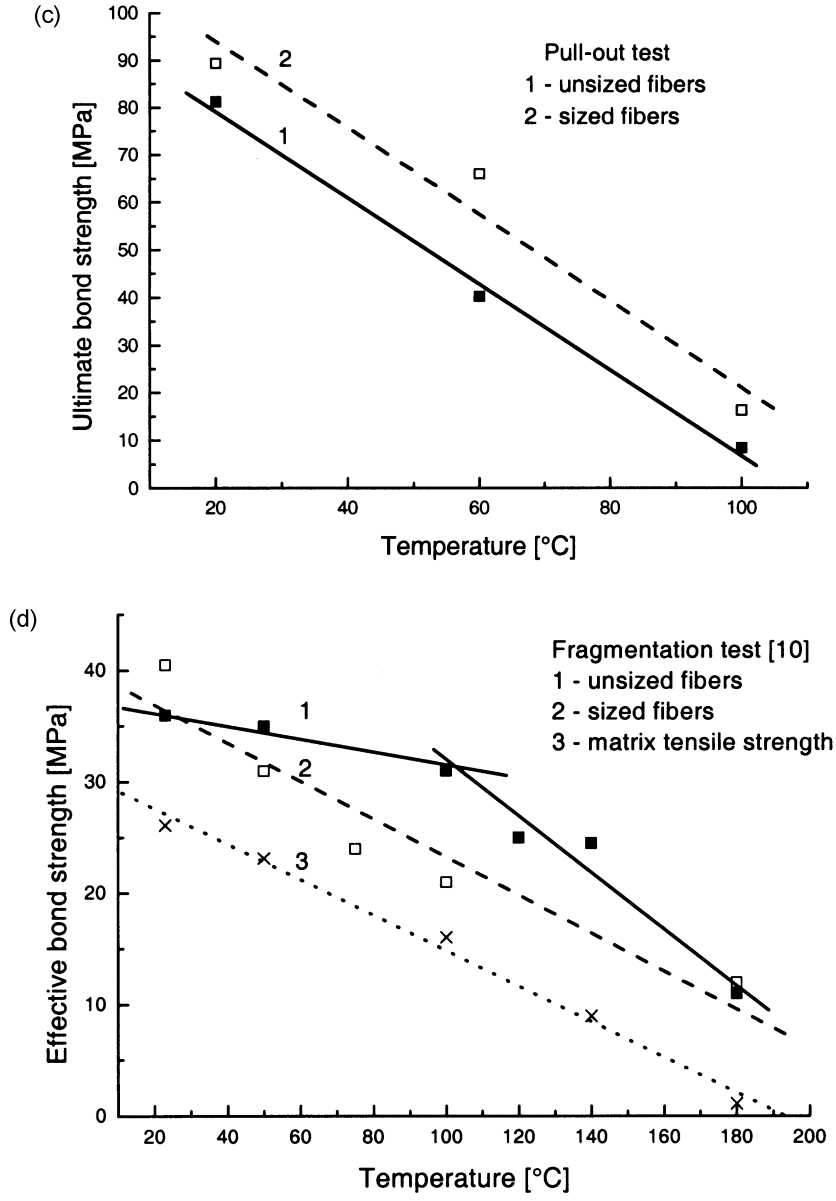

FIGURE 7 (*continued*).

First of all, we should note that the failure activation energy values for all pull-out and push-out specimens (except those with unsized fibres in the push-out tests) were similar, equal to 110–120 kJ/mol, or 1.15–1.25 eV per bond. For the sized graphite-epoxy samples tested using the fragmentation test [10], U_0 was about 150 kJ/mol (1.6 eV). These values are of the order of typical energies of chemical bonds ($\approx$ 240 kJ/mol, or 2.5 eV, for C–C and C–Si bonds [22]) but somewhat lower. Thus, we can infer that during specimen loading, chemical bonds are stressed and finally break due to thermal fluctuations. For some pure polymers, the breakage of chemical bonds during mechanical failure was proved independently, using techniques of electron paramagnetic resonance, IR spectroscopy, and mass spectroscopy [20, 21]. In all probability, chemical bonds also break when an adhesional joint fails, though it is impossible to decide solely from the U_0 value whether interfacial adhesional failure or cohesional failure through the matrix takes place.

The γ parameter has dimensions of volume (m^3). It has been shown that if the stress in the specimen is distributed uniformly, the γ value should be close to the volume of an atom (in the case of chemical bond breakage) [16–19]. Experimental γ values are typically 10 to 1000 times greater than the atomic volume, which can be attributed to stress concentration within the specimen [16–19]. Table 2 shows that, indeed, the typical values of $\gamma^{1/3}$ (8–10 Å) exceed the atomic size by several times.

There is also another possible case when γ is many times greater than the atomic volume. This takes place when the strength of the specimen is determined by interchain (intermolecular physical) interaction rather than by chemical bonds in the main chain. The intensity of this intermolecular interaction depends on the species of atoms in the polymer chains and the distance between the neighboring chains (macromolecules), and the γ parameter is proportional to the effective volume corresponding to an elementary failure event [21]. In all probability, this case (breakage of physical intermolecular bonds) takes place in the failure of samples with unsized fibres under a stress state that includes compression (the push-out and fragmentation tests). The calculated γ values for this case ($\sim 10^{-26}\,m^3$) are greater by an order of magnitude than the γ values for other specimens, which implies the "delocalized" failure, i.e., simultaneous breakage of several physical bonds. As a consequence, the calculated U_0 value for these specimens (about 3 eV in Table 2) is substantially overestimated. For a correct estimation of the energy of physical bonds, this energy should be related to the same characteristic volume, γ, observed for other specimens of the same nature [21]. Because the energy of physical

bonds is an order of magnitude smaller, it can be estimated as $U_{0p} \approx U_0/10 \approx 0.3-0.4$ eV, which corresponds to the energy of physical interaction between two condensed media due to van-der-Waals and acid-base interactions [23], or the characteristic activation energy for the viscous flow of polymers [24]. In an epoxy–glass (carbon) fibre system, this type of failure can be observed either for interfacial shear (with purely physical bonding) or for plastic yielding of the matrix near the fibre surface (Figure 5, Table 1). The latter case is more probable, because the interfacial shear would be accompanied by the breakage of chemical bonds, whose presence in this system has been shown before [25] and indirectly confirmed in this work. (The U_0 values presented here are for the same material system, but are generated using the pull-out technique).

The analysis above demonstrates the efficiency of glass fibre sizing (improvement of fibre adhesion to an epoxy matrix). It also shows that the pull-out test is a better tool for measuring adhesion in fibre–polymer systems than the fragmentation and push-out tests, because in the last two tests the failure mechanism can be substantially non-adhesional. The calculated values of the activation energy for the failure process of adhesional joints of both sized and unsized glass fibres with an epoxy matrix unambiguously demonstrate that the bond strength of glass-epoxy contacts is determined by "strong" (chemical) interactions.

CONCLUSIONS

We have compared bond strengths of differently-sized glass fibres derived from either pull-out or push-out tests at ambient and elevated temperatures. For APS-sized glass fibres, the values of both tests are in a good agreement and decrease continuously with increasing temperatures, indicating that the bond strength of glass-epoxy contacts is determined by "strong" (chemical) interactions. The failure activation energy values for all pull-out and push-out specimens were similar and equal to 110−120 kJ/mol, or 1.15−1.25 eV per bond. These values were in reasonable agreement with fragmentation test data for sized graphite–epoxy samples [10], from which activation energies of about 150 kJ/mol (1.6 eV) were determined. These values are close to typical values of activation energies for chemical reactions.

The only exception was found with unsized fibres. Due to the different failure mechanisms in the push-out and pull-out tests, the failure can be either interface-controlled or matrix-controlled, depending on the testing temperature in the push-out test. However,

the pull-out test proved to be a better tool for adhesion estimation in fibre-polymer systems.

Experimental proof in the form of AFM fractographs for pulled-out fibres documented very smooth fracture surfaces in pull-out tests for unsized fibre/epoxy specimens, whereas all push-out fibre fracture images were dominated by extensive plastic deformation of the matrix along with fibre-matrix interfacial debonding. With increasing push-out temperature, the roughness data are probably reduced due to significant and localised easier plastic deformation within the interphase region. The fracture surfaces of sized fibres revealed more than doubled roughness compared with unsized ones, a result attributed to strong interfacial adhesion.

REFERENCES

[1] Miller, B., Muri, P., and Rebenfeld, L., *Composites Sci. Technol.* **28**, 17 (1987).
[2] Dutschk, V., Pisanova, E., Mäder, E., and Schneider, K., *Composite Interfaces* **6**, 121 (1999).
[3] Mandell, J. F., Chen, J. H., and McGarry, F. J., *Int. J. Adhesion Adhesives* **1**, 40 (1980).
[4] Ho, H., and Drzal, L. T., *Composites* **27A**, 961 (1996).
[5] Zhandarov, S. F., and Pisanova, E. V., *Composites Sci. Technol*. **57**, 957 (1997).
[6] Gorbatkina, Yu. A., *Adhesive Strength of Polymer–Fibre Systems* (Ellis Horwood, NY-London, 1992).
[7] Outwater, J. D., and Murphy, M. C., *Modern Plastics* **47**, 160 (1970).
[8] Scheer, R. J. and Nairn, J. A., *J. Adhesion* **53**, 45 (1995).
[9] Mäder, E., Zhou, X.-F., Pisanova, E., Zhandarov, S. and Nutt, S. R., *Adv. Composites Lett*. **9**, 195 (2000).
[10] Wimolkiatisak, A. S., and Bell, J. P., *Polymer Composites* **10**, 162 (1989).
[11] Pisanova, E., Zhandarov, S., and Schneider, K., *J. Macromol. Sci. Phys.* **B38**, 945 (1999).
[12] Nayeh, A. H. *Fibre Sci. Technol*. **701**, 195–209 (1997).
[13] Kelly, A., and Tyson, W. R., *Mech. Phys. Solids* **13**, 329 (1965).
[14] Gao, S., and Mäder, E. *Composites Part A* **33**, 550–576 (2002).
[15] Pisanova, E., Zhandarov, S., Mäder, E., Ahmad, I., and Young, R. J., *Composites* **A32**, 435 (2001).
[16] Zhurkov, S. N., and Narzulaev, B. N., *J. Techn. Phys. (USSR)* **23**, 1677 (1953).
[17] Zhurkov, S. N., and Tomashevsky, E. E., *J. Techn. Phys. (USSR)* **25**, 66 (1955).
[18] Zhurkov, S. N., and Abasov, S. A., *High Molecular Weight Compounds* **3**, 441 (1961).
[19] Zhurkov, S. N., and Abasov, S. A., *High Molecular Weight Compounds* **4**, 1703 (1962).
[20] Regel, V. R., Slutsker, A. I., and Tomashevsky, E. E., *Advances in Physics (USSR)* **106**, 193 (1972).
[21] Regel, V. R., Slutsker, A. I., and Tomashevsky, E. E., *Kinetic Nature of the Strength of Solids* (Nauka Publishers, Moscow, 1974).
[22] Wake, W. C., *Adhesion and the Formulation of Adhesives* (Applied Science Publishers, London–New York, 1982).

[23] Lee, L.-H. In: *Contact Angle, Wettability and Adhesion*, Mittal, K. L., Ed. (VSP, Utrecht, The Netherlands, 1993), p. 45.
[24] Privalko, V. P., *Molecular Structure and Properties of Polymers* (Khimia Publishers, Leningrad, 1986).
[25] Pisanova, E., and Mäder, E., *J. Adhesion Sci. Technol.* **14**, 415 (2000).